ACS OMEGA

http://pubs.acs.org/journal/acsodf

Article

Thermodynamic Analysis of *In Situ* Underground Pyrolysis of Tar-Rich Coal: Primary Reactions

Fu Yang,[‖] Kun Gao,[‖] Zunyi Yu, Li Ma, Husheng Cao, Panxi Yang, Wei Guo, Jie Zhang, Bolun Yang, and Zhiqiang Wu*

Cite This: *ACS Omega* 2023, 8, 18915−18929

Read Online

ACCESS | Metrics & More | Article Recommendations

ABSTRACT: *In situ* underground pyrolysis of tar-rich coal is significant for alleviating the scarcity of oil and gas resources and realizing the green and efficient development and utilization of coal in China. Tar-rich coal is often subjected to high axial pressure, surrounding pressure, and pore pressure in the *in situ* underground pyrolysis environment. Consequently, laboratory simulation conditions are difficult to meet the actual needs. This paper conducts a thermodynamic study of the pyrolysis characteristics of tar-rich coal under an *in situ* environment. Typical thermodynamic functions of tar-rich coal, including the standard enthalpy of formation, standard formation Gibbs free energy, and standard entropy, were determined. Ten representative primary reactions were constructed with typical tar-rich coal pyrolysis oil components as a guide. The Gibbs free energy and equilibrium constant change laws of the above reactions were analyzed for pyrolysis temperatures from 200 to 800 °C and pyrolysis pressures from atmospheric pressure to 10 MPa. The results showed that the standard enthalpy of formation of tar-rich coal was −72.27 kJ·mol^{-1}, the standard entropy was −37.79 J·mol^{-1}·K^{-1}, and the standard formation Gibbs free energy was −60.01 kJ·mol^{-1}. When the reaction pressure increased from atmospheric pressure to 10 MPa, the thermodynamically feasible initial temperature fractions of the primary reaction of tar-rich coal pyrolysis all showed different degrees of increase. In the underground environment, the initial temperature of the primary reaction of *in situ* underground pyrolysis of tar-rich coal moves to a higher-temperature gradient to some extent, so the adjustment of the reaction temperature and pressure could guide the directional regulation of the *in situ* underground pyrolysis products of tar-rich coal.

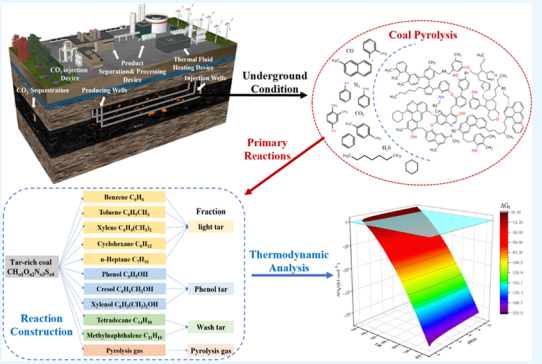

1. INTRODUCTION

Coal, an important component of world energy consumption, accounted for 27.2% of the world's total primary energy consumption in 2020.[1] China's share of coal in the total primary energy consumption in 2021 is about 56%.[2] Based on China's energy structure characteristics, it will be difficult to change the status of coal as the main energy source for a long time.[3] The degree of oil and gas dependence on foreign trade reached 72 and 44%, respectively, in 2021.[4] Tar-rich coal refers to coal with tar dry basis yield of 7−12%.[5] The most typical feature of tar-rich coal is its many hydrogen-rich structures. The structure mainly refers to the weak bond structure attached to the edge of the condensed aromatic nucleus or the branched chain and side chain of the aromatic nucleus and the bridge bond between the aromatic nucleus.[6] They are mainly composed of methyl, methylene, methine, and quaternary carbon, which could be decomposed and volatilized to produce tar and gas during pyrolysis.[7,8] Therefore, tar-rich coal is a special coal resource integrating coal, oil, and gas properties. Tar-rich coal accounts for more than 85% of the 170 billion tons of coal identified in Shaanxi, which could extract about 14.5 billion tons of tar.[6] Therefore, realizing efficient utilization of tar-rich coal is of great significance in alleviating the urgent need for China's tight oil and gas resources.

Currently, the main utilization of tar-rich coal is dominated by conventional ground pyrolysis, through underground mining and transporting coal to the ground, followed by washing and processing into ground pyrolysis equipment to convert it into tar, gas, and semicoke products. Ground pyrolysis has problems such as overcapacity of pyrolysis semicoke and air and water pollution. In addition, the coal preparation and coking sections emit a large amount of dust, and each ton of coke produced emits about 4900 m^3 of gas, causing serious environmental pollution.[9]

Received: February 27, 2023
Accepted: April 28, 2023
Published: May 15, 2023

The schematic diagram of underground *in situ* pyrolysis is shown in Figure 1, including a hot fluid heating device,

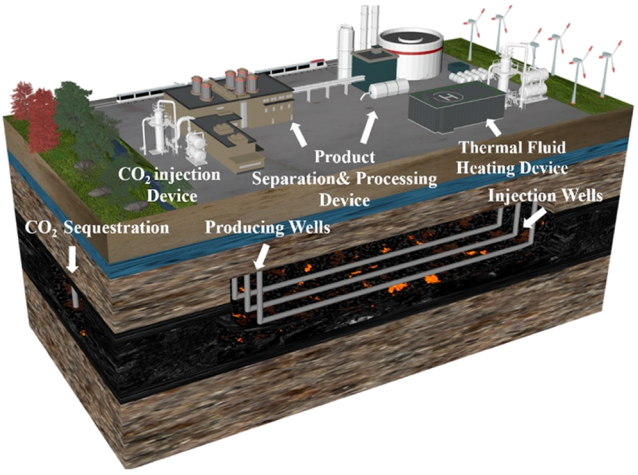

Figure 1. Schematic diagram of *in situ* underground pyrolysis.

multiple production wells and injection wells, a product separation processing device, and a CO_2 injection device. *In situ* underground pyrolysis is a technology in which coal is not mined but converted directly underground by pyrolysis through transferring heat of high-temperature and high-pressure heat fluids by injection wells. The resulting oil and gas products are imported to ground equipment through production wells, subsequently separated, and further processed. In addition, CO_2 can be injected into the underground semicoke environment through the CO_2 injection device for geological storage of CO_2. Compared with conventional ground pyrolysis technology, *in situ* underground pyrolysis has the advantages of a small footprint, prevention of ground collapse, low carbon footprint, and low mining cost. Therefore, *in situ* underground pyrolysis of tar-rich coal has a broad prospect, and realizing the efficient utilization of tar-rich coal is of great significance to alleviate the urgent demand of oil and gas resources in China and to realize the green and efficient utilization of coal in China.

One of the most significant differences between *in situ* underground pyrolysis and ground pyrolysis of tar-rich coal is that the deeper coal bodies are often subjected to higher axial, circumferential, and pore pressures. In the last few decades, the pyrolysis of coal under high pressure has been extensively studied, and the effects of pressure on pyrolysis tar and pyrolysis volatiles have been observed. Table 1 summarizes the published experimental studies on coal pyrolysis under high pressure.

Figure 2 shows the variation of tar and volatile fraction yields with high pressure in ground coal pyrolysis experiments. With increasing pressure, both tar and volatile fraction yields tend to decrease. The increase in pyrolysis pressure will lead to an increase in the residence time of the volatile fraction in the pyrolysis process, which promotes the degree of the radical polymerization reaction and carbon deposition inside the particles, thus blocking the pore structure and further reducing the diffusion ability of product molecules, resulting in the prolongation of the secondary reaction of initial pyrolysis products,[28] so that some primary pyrolysis products react with semicoke and gaseous products.[29]

Research on *in situ* underground pyrolysis of coal is still in the laboratory stage. The University of Utah has studied the pyrolysis behavior of coal in the underground environment using chemical permeation devolatilization (CPD) model simulations and a high-pressure reactor.[30,31] The results indicate that the product of subsurface coal thermal treatment technology is mainly light crude oil.[32,33] Taiyuan University of Technology studied the physical characteristics of coal during pyrolysis under high-temperature triaxial stress using an *in situ* developed high-temperature and high-pressure rock triaxial testing machine,[34] and the porosity of coal decreased with increasing pore pressure under *in situ* underground pyrolysis.[35,36] Duan et al.[37] used a high-temperature and high-pressure rheometer to study the pyrolysis characteristics of coal under different stress conditions. The results showed that the gas and semicoke yields increased with increasing stress, while the tar yield decreased. The current research mainly discusses the distribution of *in situ* underground pyrolysis products and does not involve mechanistic analysis.

Table 1. Published Experimental Studies On Coal Pyrolysis At Pressure

coal type(s)	pressure range (MPa)	temperature (°C)	heating rate (K/s)	particle size	experimental apparatus	references
Loy Yang lignite	0.1−6	700	1000	106−150 μm	wire-mesh reactor	10
Taiheiyo coal	0.1−3	800	25	75−150 μm	drop tube furnace reactor	11
Illinois No. 6	0.1−7	850	1000	106−150 μm	wire-mesh reactor	12
Tilmanstone	0.1−7	700	1000	106−150 μm	wire-mesh reactor	13
Bituminous coal	0.1−7	700	1000		wire-mesh reactor	14
German coal	0.1−10	1000	3−200	0.2−0.315 mm	wire-net reactor	15
Linby coal	0.1−3	600	625	100−150 pm	wire-mesh reactor	16
Pittsburgh No. 8	0.1−7	700	1000		wire-mesh reactor	17
Tianzhu coal	0.1−3	650	10	0.5−1 mm	heating furnace	18
Daw Mill coal	0.1−3	1000	1000	106−150 μm	wire-mesh reactor	19
Daw Mill coal	0.1−3	1000	1000	106−150 μm	wire-mesh reactor	20
Westerholt coal	0.1−4	1000	5	0.1−2 mm	thermogravimetric analyzer	21
Godavari coal	0.1−7	650	3	0.5−0.8 mm	flow-through reactor	22
Gas coal	0.1−7	1000	3	100 μm	thermobalance	23
Zhundong coal	0.1−3	800	20	106−150 μm	wire-mesh reactor	24
Berau coal	0.1−5	800	2000	75−150 mm	free-fall pyrolyzer	25
Yanchang coal	0.1−3	600	20	96−150 μm	pressurized fixed bed	26
Linby coal	0.1−3	700	1000	100−150 μm	hot-rod reactor	27

https://doi.org/10.1021/acsomega.3c01321
ACS Omega 2023, 8, 18915−18929

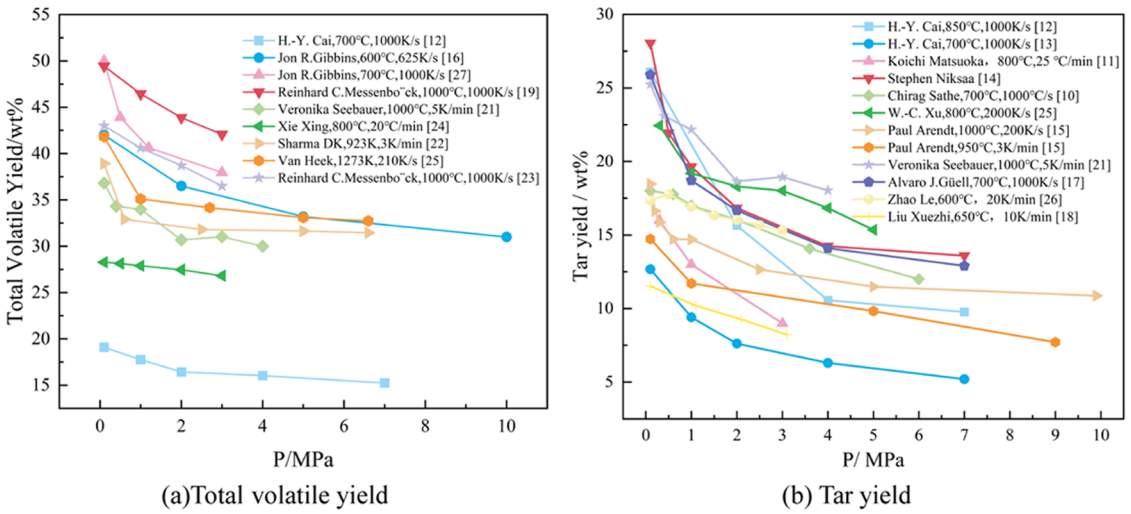

Figure 2. Variation of pyrolysis tar yield and volatile fraction yield with pressure.

The thermodynamic analysis is widely used in the coal chemical industry as an important part of the study of the chemical reaction process. Cheng et al.[38] used the Gibbs minimum free energy method to carry out a thermodynamic analysis of direct methane production from coal, and the results showed that 500−700 °C and 5−10 MPa are more suitable reaction conditions for the system. Lv et al.[39] carried out a thermodynamic analysis of acetylene production from coal under different atmospheres by constructing the thermodynamic reaction function for acetylene production from coal plasma pyrolysis. The results showed that acetylene production from coal under a H_2 atmosphere is thermodynamically feasible. Therefore, thermodynamic analysis is an important tool for studying the distribution of reaction products. Based on the thermodynamic analysis, it is possible to understand the possibility of the reaction, predict the distribution of products, and select the best experimental conditions for synthesizing target products.

This paper studies the thermodynamic analysis of *in situ* underground pyrolysis of tar-rich coal. First, the thermodynamic functions, including standard enthalpy of formation, standard formation Gibbs free energy, and standard entropy of tar-rich coal were constructed. Second, the reaction of *in situ* underground pyrolysis was constructed, which includes the reaction of tar-rich coal to produce light oil, phenol oil, washed oil, and other components in one reaction, and the change of Gibbs free energy of one reaction and the variation law of reaction equilibrium constant with reaction temperature and pressure were calculated. The results obtained provide basic data for the evaluation of the feasibility of *in situ* underground pyrolysis technology and provide theoretical guidance for the practical production of *in situ* underground pyrolysis of tar-rich coal.

2. MODELS AND METHODS

2.1. Construction Method of Thermodynamic Function for Tar-Rich Coal. *2.1.1. Calculation of the Standard Enthalpy of Formation.* Tar-rich coal is widely distributed in Jurassic coal fields in northern Shaanxi and Triassic coal fields in northern Shaanxi, with more than 150 billion tons of resources. Thus, Shenfu coal was selected as a representative of tar-rich coal. The molecular formula of coal was initially set as $CH_{\alpha 1}O_{\alpha 2}N_{\alpha 3}S_{\alpha 4}$ according to the main elements of Shenfu coal (Table 2), and the standard enthalpy of formation of coal was calculated based on the reactants obtained from the chemical

Table 2. Proximate and Ultimate Analyses of Tar-Rich Coal and Its Molar Ratio to C

Proximate Analysis (wt %)			
M_{ad}	A_d	V_{daf}	FC_{ad}
5.3	4.82	41.49	52.75
Ultimate Analysis (wt % daf)			
C	H	O[a]	N	S
68.86	4.40	25.04	0.82	0.88
Stoichiometry				
number of chemical measures	1	α_1	α_2	α_3	α_4
molar ratio of C (%)	1	0.761	0.273	0.010	0.005

[a]Obtained by-difference.

reaction equation of coal combustion and the reaction heat of coal combustion.

$$CH_{\alpha_1}O_{\alpha_2}N_{\alpha_3}S_{\alpha_4} + \left(1 + \frac{\alpha_1}{4} + \alpha_4 - \frac{\alpha_2}{2}\right)O_2 \rightarrow CO_2 + \frac{\alpha_1}{2}H_2O + \frac{\alpha_3}{2}N_2 + \alpha_4 SO_2 \quad (1)$$

where α_1, α_2, α_3, and α_4 are the molar ratios of H, O, N, and S elements to C elements in Shenfu tar-rich coal determined from the results of the coal elemental analysis in Table 1, respectively.

$$\Delta H_f(\text{coal}) = \sum_{i=1}^{4} v_i \Delta H_f(\text{'Reaction products'}) - Q \quad (2)$$

For the complete combustion reaction of coal, the products mainly include H_2O, CO_2, SO_2, and N_2, and their standard enthalpies of formation of production are shown in Table 3.[40]

Table 3. Standard Enthalpy of Formation of Some Reactants and Products

reactants	O_2	CO_2	H_2O	N_2	SO_2
$\Delta_f H_m^{\ominus}$ (kJ·mol^{-1})	0	−393.51	−241.83	0	−296.90

https://doi.org/10.1021/acsomega.3c01321
ACS Omega 2023, 8, 18915−18929

The heat of reaction for the combustion reaction of coal can be calculated by the following three empirical equations (eqs 3−5):[41]

$$Q = -[1 + 0.15 \times O + 7837.67 \times C + 33888.89 \times (H - O/8) + 3823.75 \times S] \times \frac{4.18}{1000} \times \frac{(100 - ash)}{100} \quad (3)$$

$$Q = -[33.823 \times C + 144.25 \times ((H - O/8) + 9.419 \times S] \times \frac{\frac{(100 - ash)}{100}}{1000} \quad (4)$$

$$Q = -(80 \times C + 310 \times H + 15 \times S - 25 \times O) \times \frac{4.18}{1000} \times (100 - ash) \quad (5)$$

2.1.2. Calculation of Standard Entropy. Due to the complexity of coal composition and structure, it is usually difficult to obtain accurate thermodynamic data. Based on the theory of chemical thermodynamics, the standard formation Gibbs free energy can be calculated by the standard enthalpy of formation and the standard entropy. The standard enthalpy of formation of tar-rich coal has been calculated. According to the results of elemental analysis, the molecular formula of tar-rich coal can be constructed, and the reaction equation of coal formation from related elements can be constructed, as shown in eq 6.

$$C(s) + 0.3805H_2(g) + 0.1365O_2(g) + 0.005N_2(g) + 0.005S(s) \rightarrow CH_{0.761}O_{0.273}N_{0.01}S_{0.005} \quad (6)$$

Based on its empirical thermodynamic properties and thermodynamic analyses of model compounds similar to coal pyrolysis products, this paper calculates the standard entropy from related simple substances to coal through a series of reversible steps, as shown in Figure 3 and the following formula:[39]

$$\Delta_r S_m^{\ominus} = \sum_{i=4}^{4} \Delta S_i \quad (7)$$

Step 1: The graphitic carbon C(s) and solid sulfur S(s) reached the sublimation temperature by reversible isobaric heating and sublimated to the gaseous state. Hydrogen, nitrogen, and oxygen are heated to the highest temperature for gas dissociation at reversible isobaric temperatures, with nitrogen dissociation temperatures up to 6900 K (based on DFT calculations). The reversible isobaric temperature rise and the entropy change of the phase change are calculated as follows:

$$\Delta S = \int_{T_i}^{T_2} \frac{v_i C(i)_{p,m}}{T} dT + \frac{v_i \Delta H_i}{T_i} \quad (8)$$

where v_i is the stoichiometric number, $C(i)_{p,m}$ is the heat capacity at constant pressure ($J \cdot mol^{-1} \cdot K^{-1}$), and ΔH_i is the heat of phase transition ($kJ \cdot mol^{-1}$), where the sublimation temperature of graphite was 3970.15 K. T_i is the phase transition temperature (K), so the calculation of ΔS_1 is shown in eq 9:

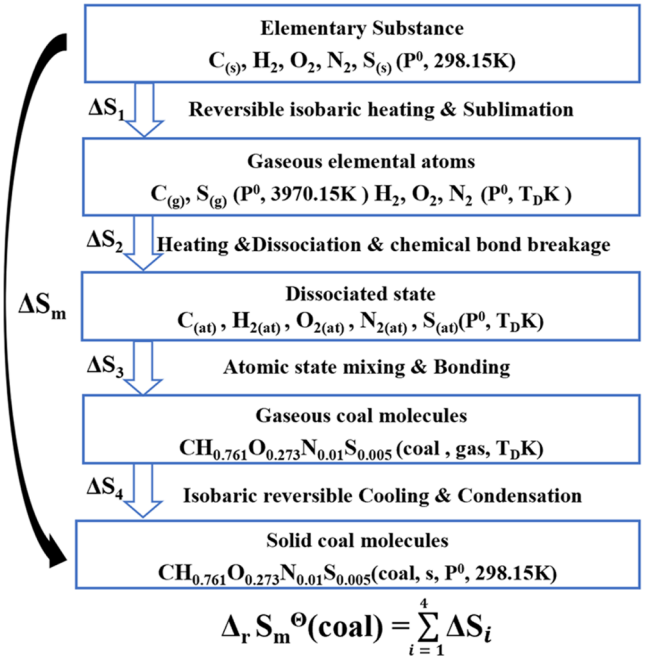

Figure 3. Schematic diagram of standard entropy calculation steps.

$$\Delta S_1 = \int_{298.15}^{3970.15} \frac{v_c C(c)_{p,m} + v_s C(s)_{p,m}}{T} dT + \int_{298.15}^{6900} \frac{v_{H_2} C(H_2)_{p,m} + v_{N_2} C(N_2)_{p,m} + v_{O_2} C(O_2)_{p,m}}{T} dT + \frac{v_s \Delta H(S)}{T(S)} + \frac{v_c \Delta H(C)}{T(C)} \quad (9)$$

Step 2: The gaseous graphite C(g) and sulfur S(g) are heated to the highest dissociation temperature of the system, and the chemical bonds of the three gas molecules are broken, transforming them into atomic states. Assuming that the transition from a gas state to an atomic state can also be regarded as a phase transition process, the entropy change is calculated by the entropy calculation formula of the phase transition process, as shown in the following

$$\Delta S = \int_{T_i}^{T_2} \frac{v_i C(i)_{p,m}}{T} dT + \frac{v_i \Delta H_i}{T_D K} \quad (10)$$

where ΔH_i is the chemical bond energy of the gas molecule ($kJ \cdot mol^{-1}$); each chemical bond energy is shown in Table 4.[40]

Table 4. Bond Dissociation Energy under Standard Conditions

bond	H−H	O=O	N≡N
dissociation energy ($kJ \cdot mol^{-1}$)	436	498	945

$T_D K$ is the highest dissociation temperature (K), so the calculation of ΔS_2 is shown in eq 11:

$$\Delta S_2 = \int_{3970.15}^{6900} \frac{v_c C(c)_{p,m} + v_s C(s)_{p,m}}{T} dT + \frac{v_{O_2} \Delta H(O{=}O)}{T_D K} + \frac{v_{H_2} \Delta H(H{-}H)}{T_D K} + \frac{v_{N_2} \Delta H(N{\equiv}N)}{T_D K} \quad (11)$$

https://doi.org/10.1021/acsomega.3c01321
ACS Omega 2023, 8, 18915−18929

Step 3: Several atomic substances are reversibly mixed at isothermal, isobaric pressure, and they form chemical bonds. The enthalpy changes of the mixing process and the chemical bond formation process are shown in eqs 12 and 13:

$$\Delta S_{\mathrm{mix}} = -R \sum_i n_i \ln x_i \tag{12}$$

$$\Delta S = \sum_i X_i \frac{\Delta_{\mathrm{D}} H_i}{T_i} \tag{13}$$

where R is the molar gas constant (8.314 J·mol^{-1}·K^{-1}), n_i and x_i are the amount of component substance and the mass fraction of substance, respectively, X_i is the proportion of main chemical bonds in coal, $\Delta_{\mathrm{D}}H_i$ is the chemical bond energy (kJ·mol^{-1}), and T_i is the dissociation temperature (K).

The main covalent bonds of coal are determined according to the Shinn model, and the proportions are shown in Table 5.[42] The energy change of the chemical bond formation process can take the negative value of the dissociation energy of the corresponding chemical bond, so the calculation of ΔS_3 is shown in eq 14:

Table 5. Proportion of Chemical Bonds under Standard Conditions

bond	C−C	C=C	C−H	C=O	C−O	C=N	C−S
proportion	1.1	1	0.8	0.04	0.05	0.002	0.001

$$\Delta S_3 = -R \sum_i n_i \ln x_i + \sum_i X_i \frac{\Delta_{\mathrm{D}} H_i}{T_i} \tag{14}$$

Step 4: As a mixture, coal does not have a single sublimation temperature. Coal begins to release volatiles at about 200 °C, releasing a large amount of volatiles as the temperature increases. In the later stage, the condensation reaction is the final graphite-type carbon with a regular structure. Therefore, the sublimation temperature of graphite and the sublimation heat are used to replace coal carbon, and coal is first reduced from the highest temperature of the system to the sublimation temperature. The isothermal reversible phase transition is carried out, and finally, the temperature is reduced to the standard condition, as shown in the following:

$$\Delta S = \int_{T_2}^{T_3} \frac{C(\mathrm{coal})_{\mathrm{p,m}}}{T}\,\mathrm{d}T - \frac{v_{\mathrm{c}}\Delta H(C)}{T(C)} + \int_{T_1}^{T_2} \frac{C(\mathrm{coal})_{\mathrm{p,m}}}{T}\,\mathrm{d}T \tag{15}$$

The following equation gives the standard enthalpy of formation of production of coal as a function of temperature:

$$H_{\mathrm{coal}} = \frac{R}{M_{\mathrm{a}}}\left[380 g_0\left(\frac{380}{T}\right) + 3600 g_0\left(\frac{3600}{T}\right)\right] \tag{16}$$

where $g_0(x) = \frac{1}{\exp(x)-1}$, M_{a} is the average relative atomic mass of coal, and $C_{\mathrm{p}} = \left(\frac{\partial H}{\partial T}\right)_{\mathrm{p}}$ is the constant pressure heat capacity of the substance; thus, the calculation of ΔS_4 is shown in eq 17:

$$\Delta S_4 = -\frac{R}{M_{\mathrm{a}}} \int_{298.15}^{6900} \frac{1}{T^3}\left\{380\left[g_0\left(\frac{380}{T}\right)\right]^2 \exp\left(\frac{380}{T}\right) + 3600\left[g_0\left(\frac{3600}{T}\right)\right]^2 \exp\left(\frac{3600}{T}\right)\right\} \mathrm{d}T - \frac{v_{\mathrm{c}}\Delta H(C)}{T(C)} \tag{17}$$

2.1.3. Calculation of the Standard Formation Gibbs Free Energy. The standard formation Gibbs free energy of tar-rich coal is calculated by the standard enthalpy of formation and the standard entropy, as shown in eq 18.

$$\Delta_{\mathrm{f}} G_{\mathrm{m}}^{\ominus} = \Delta_{\mathrm{f}} H_{\mathrm{m}}^{\ominus} - T\Delta_{\mathrm{r}} S_{\mathrm{m}}^{\ominus} \tag{18}$$

2.2. Primary Reaction Construction and Thermodynamic Analysis Method for *In Situ* Underground Pyrolysis of Tar-Rich Coal. *2.2.1. Primary Reaction Construction.* Primary reactions of coal play an important role in the cleavage of organic matter. The main cleavage reactions that occur in primary pyrolysis of coal include −CH_2−, −CH_2−CH_2−, −CH_2−O−, −O−, −S−, and other bridge bond breakage to generate free radical fragments; cleavage of fatty side chains to create gases such as CH_4 and C_2H_4; cleavage of oxygen-containing functional groups; and cleavage of low molecular compounds.[43] As an important product of the pyrolysis of tar-rich coal, this paper starts from the directional regulation of tar products based on the *in situ* underground pyrolysis of tar-rich coal. First, tar is classified according to the fraction of coal pyrolysis tar, as shown in Table 6[44]

In this paper, from the primary reaction of coal pyrolysis, the equation of the primary coal reaction is constructed by the simplified formula of the coal molecule $CH_{0.761}O_{0.273}N_{0.01}S_{0.005}$ obtained from elemental analysis. According to some typical components in each fraction of tar as the main reaction products and referring to a large number of coal pyrolysis experiments and molecular dynamics simulations, the reaction products are derived from the intermediate products detected in the experiment and the primary reaction products of coal pyrolysis in the simulation. As shown in Table 7, some aromatic hydrocarbons, phenols, and aliphatic hydrocarbons are selected as products to construct the primary reaction of

Table 6. Tar Fraction and Composition of Coal Pyrolysis

fraction	boiling point (°C)	main components	low-temperature tar (400−650 °C)	medium-temperature tar (650−900 °C)
light oil	<170	benzene, toluene, xylene, etc.	7.2−9.6	1.8−4.3
phenol oil	170−210	phenol, cresol, dimethyl phenol, etc.	10.3	7.6−9.5
naphthalene oil	210−230	naphthalene, dodecane, etc.	11.4	22−24
oil washing	230−300	fluorene, acenaphthene, methylnaphthalene, etc.	11.5−13.2	7.6−9.4
anthracene oil	300−360	anthracene, phenanthrene, carbazole, etc.	16.5−20	15.2−17.9
pitch	>360	aromatic compounds with more than three rings	35.7−40.2	34−36.9

https://doi.org/10.1021/acsomega.3c01321
ACS Omega 2023, 8, 18915−18929

Table 7. Some Typical Primary Reaction Products Published in the Literature

components	source type	literature
C_6H_6	pyrolysis intermediate products, simulated primary reaction product	45−49
C_7H_8	pyrolysis intermediate products, simulated primary reaction product	45−47, 49, 50
C_8H_{10}	pyrolysis intermediate products, simulated primary reaction product	45−47, 49
C_6H_{12}	pyrolysis intermediate products	45, 51
C_7H_{16}	pyrolysis intermediate products	51
C_6H_6O	pyrolysis intermediate products, simulated primary reaction product	45−48, 50
C_7H_8O	pyrolysis intermediate products, simulated primary reaction product	45, 47, 50
$C_8H_{10}O$	pyrolysis intermediate products	45, 47
$C_{14}H_{30}$	pyrolysis intermediate products	47, 51
$C_{11}H_{10}$	pyrolysis intermediate products, simulated primary reaction product	45−50

coal pyrolysis, as shown in Figure 4. The constructed reactions are as follows:

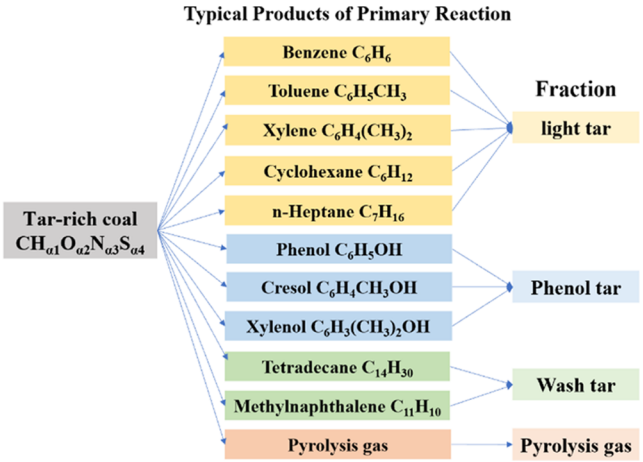

Figure 4. Classification process of main components in tar.

$$CH_{0.761}O_{0.273}N_{0.01}S_{0.005} \rightarrow 0.125C_6H_6 + 0.005N_2 + 0.005H_2S + 0.0669C + 0.091CO + 0.091CO_2 \quad (R1)$$

$$CH_{0.761}O_{0.273}N_{0.01}S_{0.005} \rightarrow 0.0939C_6H_5CH_3 + 0.005N_2 + 0.005H_2S + 0.0698C + 0.273CO \quad (R2)$$

$$CH_{0.761}O_{0.273}N_{0.01}S_{0.005} \rightarrow 0.0751C_6H_5(CH_3)_2 + 0.005N_2 + 0.005H_2S + 0.2172C + 0.091CO + 0.091CO_2 \quad (R3)$$

$$CH_{0.761}O_{0.273}N_{0.01}S_{0.005} \rightarrow 0.0626C_6H_{12} + 0.005N_2 + 0.005H_2S + 0.351C + 0.273CO \quad (R4)$$

$$CH_{0.761}O_{0.273}N_{0.01}S_{0.005} \rightarrow 0.0469C_7H_{16} + 0.005N_2 + 0.005H2S + 0.398C + 0.273CO \quad (R5)$$

$$CH_{0.761}O_{0.273}N_{0.01}S_{0.005} \rightarrow 0.1252C_6H_5OH + 0.005N_2 + 0.005H_2S + 0.101C + 0.1478CO \quad (R6)$$

$$CH_{0.761}O_{0.273}N_{0.01}S_{0.005} \rightarrow 0.0939C_6H_4CH_3OH + 0.005N_2 + 0.005H_2S + 0.1636C + 0.1791CO \quad (R7)$$

$$CH_{0.761}O_{0.273}N_{0.01}S_{0.005} \rightarrow 0.0751C_6H_3(CH_3)_2OH + 0.005N_2 + 0.005H_2S + 0.2013C + 0.1979CO \quad (R8)$$

$$CH_{0.761}O_{0.273}N_{0.01}S_{0.005} \rightarrow 0.025C_{14}H_{30} + 0.005N_2 + 0.005H_2S + 0.377C + 0.273CO \quad (R9)$$

$$CH_{0.761}O_{0.273}N_{0.01}S_{0.005} \rightarrow 0.025C_{11}H_{10} + 0.005N_2 + 0.005H_2S + 0.0275C + 0.1365CO_2 \quad (R10)$$

2.2.2. Thermodynamic Characterization Method for Primary Reactions. The Jurassic coalfield in northern Shaanxi has the most abundant oil-rich coal resources, and the Yushen mining area is the best place for coal seam burial conditions, mining conditions, coal quality, and resources. Therefore, we take the main coal-bearing strata in the Yushen mining area as the representative. The thickness of the coal seam is usually 250 m, and the burial depth is about 21−380 m.[52] According to the linear regression equation of underground vertical stress with burial depth in China's mines as $\delta_v = 0.0245H$,[53] it is presumed that the underground vertical stress is about 4.77−9.83 MPa. Thermodynamic calculations of primary reactions of tar-rich coal pyrolysis at temperatures from 200 to 800 °C and pressures from atmospheric pressure to 10 MPa are performed.

According to Kirchhoff 's equation, the relationship between the enthalpy change of the reaction and the temperature is shown in the following equation.

$$\Delta_r H_m(T_2) = \Delta_r H_m(T_1) + \int_{T_1}^{T_2} \Delta C_p \, dT \quad (19)$$

The equation for the change in heat capacity versus temperature is

$$C_p = A + 10^{-3}BT + 10^5 CT^{-2} + 10^{-6}DT^2 \quad (20)$$

Taking eqs 16 and 20 into account, the enthalpy change of the reaction during the pyrolysis of tar-rich coal is obtained as a function of temperature as follows

$$\Delta H = \Delta H_0 + AT + 10^{-3}B\frac{T^2}{2} - \frac{10^5 C}{T} + 10^{-6}D\frac{T^3}{3} - \frac{R}{M_a}\left[380g_0\left(\frac{380}{T}\right) + 3600g_0\left(\frac{3600}{T}\right)\right] \quad (21)$$

According to the Gibbs−Helmholtz formula, the change of Gibbs free energy of reaction with temperature is given by the following equation:

$$\frac{\partial(\Delta G/T)}{\partial T} = -\frac{\Delta H}{T^2} \quad (22)$$

Integrating eq 18 into the Gibbs−Helmholtz equation yields the change of Gibbs free energy of the primary reaction of tar-rich coal pyrolysis at constant pressure as a function of temperature.

https://doi.org/10.1021/acsomega.3c01321
ACS Omega 2023, 8, 18915−18929

$$\Delta G_r^{\ominus}(T) = -AT\ln T - \frac{10^{-3}B}{2}T^2 - \frac{10^{-5}C}{2T} + \frac{10^{-6}D}{6}T^3 + \frac{RT}{M_a}\left[\frac{380}{T} - \ln(e^{380/T} - 1)\right] + \frac{RT}{M_a}\left[\frac{3600}{T} - \ln(e^{3600/T} - 1)\right] + \Delta H_0 + IT \quad (23)$$

The change of Gibbs free energy of matter with temperature and pressure is

$$dG = -S\,dT + V\,dp \quad (24)$$

Additionally, $\left(\frac{\partial G}{\partial P}\right)_T = V$. Considering the small volume change of coal as a solid at different pressures, only the Gibbs free energy change of product generation is considered at different pressures, $dG = V\,dp = nRT\frac{dp}{p}$; for an ideal gas at a constant temperature, the change of Gibbs free energy versus reaction pressure is given as follows

$$G(T) = G^{\ominus}(T) + nRT\ln\frac{p}{p^{\ominus}} \quad (25)$$

The change of Gibbs free energy with pressure for the primary pyrolysis reaction at a constant temperature can be obtained as

$$\Delta G_r(T) = \Delta G_r^{\ominus}(T) + nRT\prod\ln\left(\varphi_i\frac{p_i}{p^{\ominus}}\right)^{\nu_i} \quad (26)$$

$$K_p = \exp\left[-\frac{\Delta G_r(T)}{RT}\right] \quad (27)$$

The change of the Gibbs free energy of the reaction at different pressures and the standard temperature is obtained from the above, followed by the change of the Gibbs free energy of the reaction at different temperatures and pressures and the equilibrium constant.

3. RESULTS AND DISCUSSION

3.1. Thermodynamic Functions of Tar-Rich Coal. *3.1.1. Standard Enthalpy of Formation.* The average relative atomic mass M_a of Shenfu coal was calculated to be 12.71, the molecular weight of coal was determined to be 17.44 by the simplest formula obtained from elemental analysis, and the sum of enthalpies of production of reactants was −486.99 kJ·mol^{-1}. The heat content and the standard enthalpy of production are shown in Table 8. Compared with the actual values measured by the calorimeter, the value of the empirical formula (eq 3) is the closest, so the heat content of tar-rich coal is −23.83 MJ·kg^{-1}, and the standard enthalpy of formation of tar-rich coal production is −71.27 kJ·mol^{-1}.

3.1.2. Standard Entropy and Standard Formation Gibbs Free Energy. As shown in Table 9, the standard entropy of tar-rich coal is −37.79 J·mol^{-1}·K^{-1} and the standard formation Gibbs free energy of tar-rich coal is −60.01 kJ·mol^{-1}.

Table 8. Standard Enthalpy of Formation and Heat Generation of Tar-Rich Coal

experience formula	heat generation (MJ·kg^{-1})	standard enthalpy of formation (kJ·mol^{-1})
3	−23.83	−71.27
4	−23.30	−80.50
5	−24.53	−59.05

3.2. Thermodynamic Analysis of Typical Components of Light Oil. *3.2.1. Light Aromatic Components (Benzene−Toluene−Xylene).* From Figure 5, the change of the Gibbs free energy of the primary reaction with temperature for the *in situ* underground pyrolysis of tar-rich coal to produce light aromatic components (benzene−toluene−xylene) can be seen; reactions R1, R2, and R3 at atmospheric pressure have less than 0 Gibbs free energy at 297 °C, 319 °C, and above 241 °C, respectively, and they can proceed spontaneously in this temperature range. From the change of the equilibrium constant of the reaction with temperature, it can be seen that the equilibrium constant increases with the increase of temperature, so the reactions are all heat-absorbing reactions, and the increase in temperature favors the positive proceeding of the reaction. The generation curve of benzene during coal pyrolysis generally appears as a double peak, with peak temperatures occurring at about 500 and 600 °C. The first peak of C_6H_6 generation is usually a result of the degradation and cleavage of coal macromolecular structures. In contrast, the second peak is the product of condensation reactions between aromatic and hydrogenated aromatic structures in coal.[23,54] It was reported that with the increase of pyrolysis temperature, the content of monocyclic aromatic hydrocarbons in the tar fraction decreased, while the range of polycyclic aromatic hydrocarbons and their derivatives kept increasing.[55] The heavy-fraction content increased, mainly because the higher pyrolysis temperature caused the dehydrogenation and recondensation of aromatic hydrocarbons in the tar; related scholars found the same pattern in their experiments, and as the final temperature of pyrolysis increased from 550 to 750 °C, the content of benzene substances decreased. Some even disappeared with an increase in temperature, while the naphthalene substances increased with an increase in temperature.[56] The increase in temperature at low temperatures facilitates the cleavage of macromolecular structures in coal, which leads to an increase in the content of BTX components from pyrolysis, consistent with the thermodynamic calculations. In contrast, the main reason for the deviation at high temperatures is the condensation reaction of BTX components to form PAHs.

The variation of the reaction equilibrium constant with pressure shows that the reaction equilibrium constant decreases as the pressure increases. At a pressure of 10 MPa, the Gibbs free energies of reactions R1, R2, and R3 are less than 0 at 341, 357, and 277 °C, respectively. The thermodynamically feasible temperatures of the reactions increase by 45, 38, and 36 °C, respectively, compared with atmospheric pressure, so the temperature at the beginning of the primary pyrolysis reaction moves to a higher-temperature gradient to some extent under the effect of subsurface stress. It has been shown that an increase in pyrolysis pressure decreases the yields of benzene, toluene, and xylene components in the tar. The effect of pressure on the tar yield and composition may be that an increase in pressure inhibits the volatilization of large-molecular tar components, thus causing a decrease in the amount of tar and a smaller molecular weight of the resulting tar.[57] Similar results were found experimentally by related authors, where the concentration of monocyclic aromatic compounds monotonically decreased with pressure and temperature at 600−900 °C and 0.1−4 MPa pyrolysis conditions.[58] The main reason is that the higher pyrolysis

https://doi.org/10.1021/acsomega.3c01321
ACS Omega 2023, 8, 18915−18929

Table 9. Standard Entropy and Standard Formation Gibbs Free Energy of Tar-Rich Coal

thermodynamic functions	ΔS_1	ΔS_2	ΔS_3	ΔS_4	$\Delta_r S_m^{\ominus}$	$\Delta_f G_m^{\ominus}$
$J\cdot mol^{-1}\cdot K^{-1}$ ($kJ\cdot mol^{-1}$)	111.60	231.26	−200.14	−180.53	−37.79	−60.01

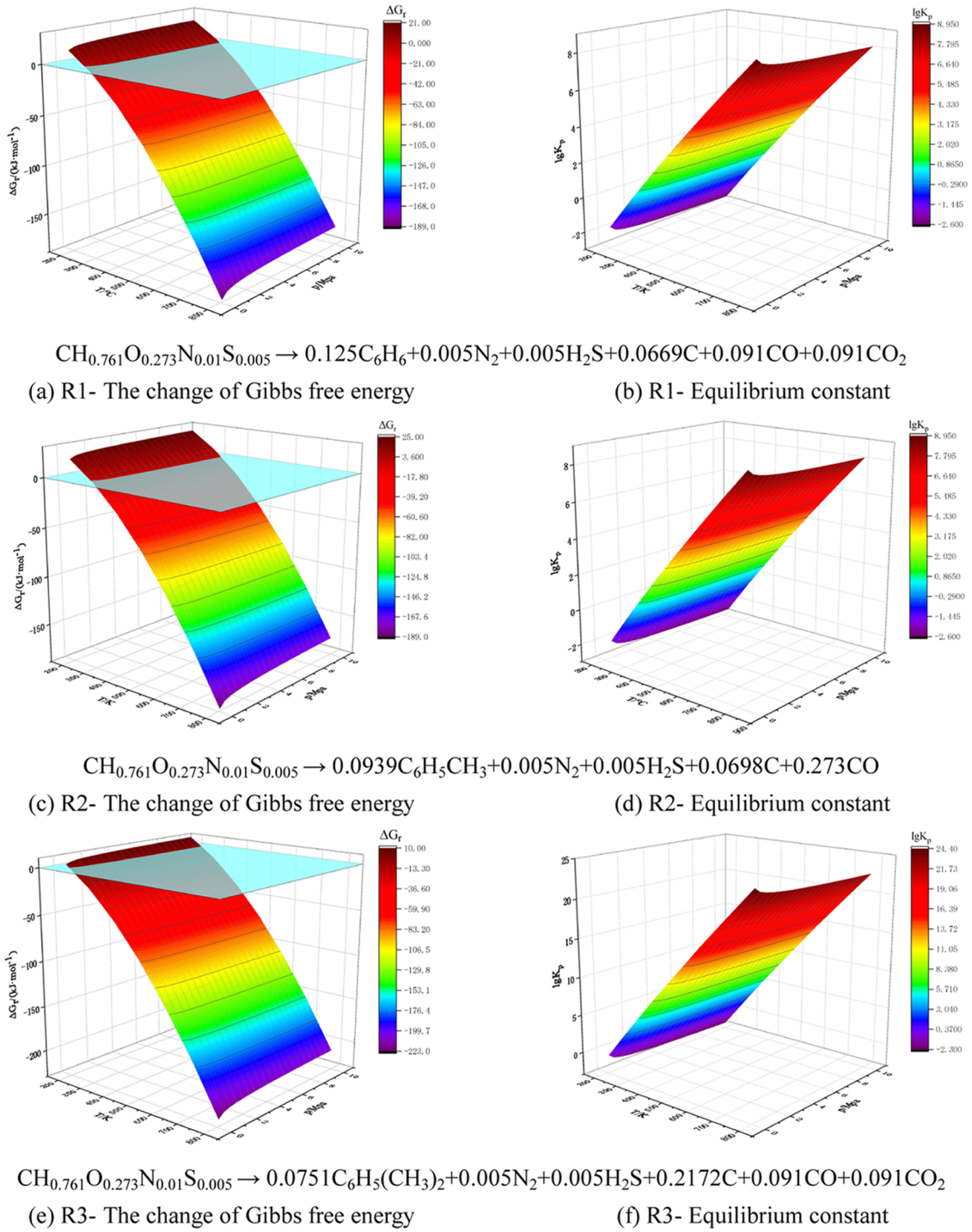

Figure 5. Effects of temperature and pressure on the change of the Gibbs free energy and equilibrium constant of light aromatic components.

pressure increases the residence time of the volatile fraction in the char particles during pyrolysis, which promotes the secondary pyrolysis reaction. Consistent with the thermodynamic findings, an increase in pressure leads to a decrease in the content of the BTX component, which is detrimental to the primary reaction but also affects the formation and release of products mainly through the promoted condensation of the BTX component.

3.2.2. Aliphatic Hydrocarbon Components. From the change of the Gibbs free energy with temperature for *in situ* underground pyrolysis of tar-rich coal to generate aliphatic hydrocarbon components in Figure 6, it can be seen that the free energies of reaction R4 to generate cyclohexane and

https://doi.org/10.1021/acsomega.3c01321
ACS Omega 2023, 8, 18915−18929

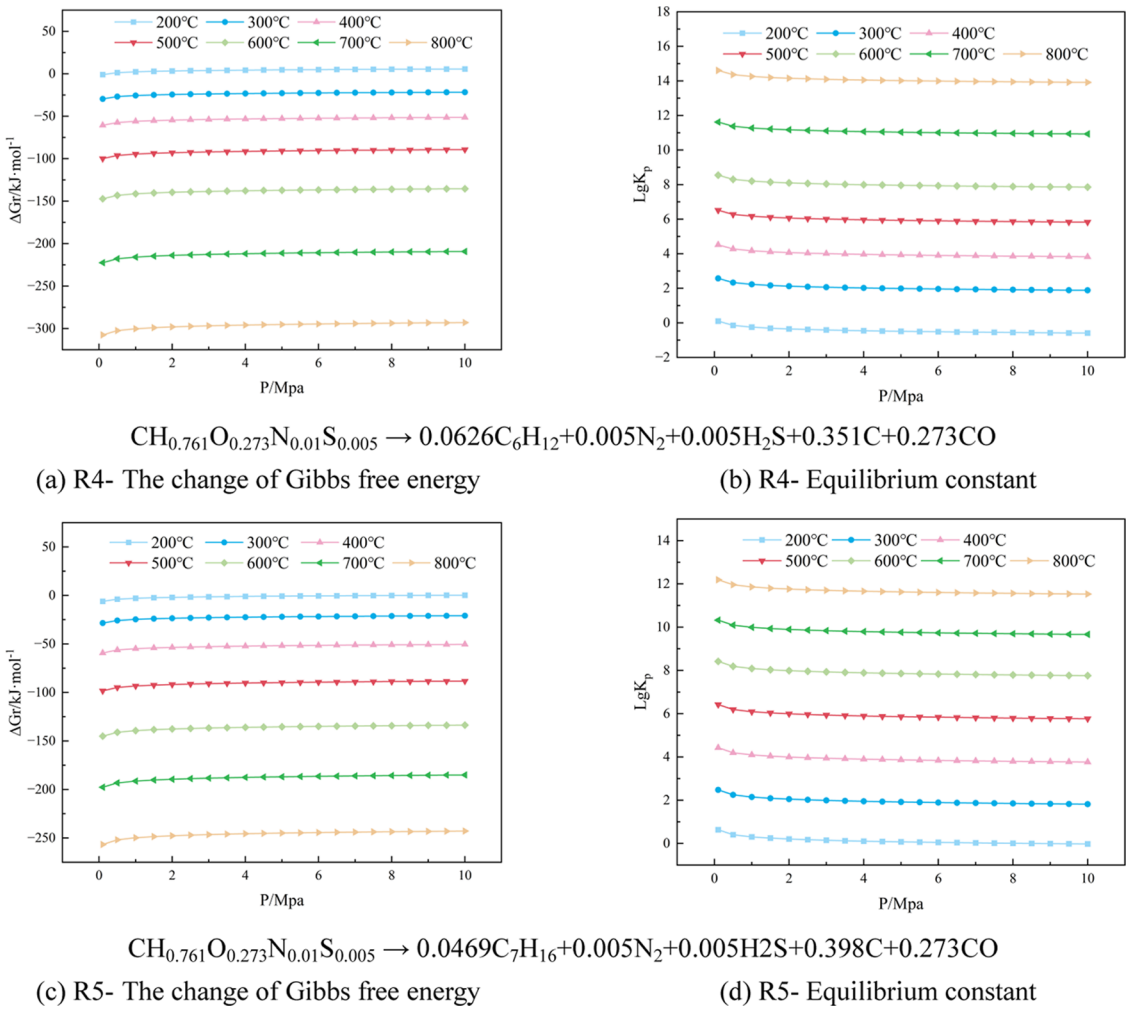

Figure 6. Effects of temperature and pressure on the change of Gibbs free energy and equilibrium constant of aliphatic hydrocarbon components.

reaction R5 to generate n-heptane at atmospheric pressure are less than 0 at 224 °C and above 205 °C, respectively, which means that the reactions can proceed spontaneously in this temperature range. The variation of the equilibrium constants of the reactions with temperature shows that the equilibrium constants increase as the temperature increases, so the reactions are all heat-absorbing reactions. The increase in temperature favors the positive proceeding of the reactions. In the process of coal pyrolysis, aliphatic hydrocarbons are mainly decomposed into tar molecular radicals by breaking the long chains or side chains, which combine with H radicals or other small-molecular radicals formed in the pyrolysis process and are analyzed in the tar with volatilization. It was found that the yield of various aliphatic compounds increased and then decreased with an increase of temperature at different pyrolysis temperatures. The maximum yield was achieved when the temperature reached 600 °C, mainly due to the bond-breaking reaction of long-chain alkanes at high temperatures to generate smaller molecules of hydrocarbons to escape.[59] The main deviation from the thermodynamic analysis stems from the fact that secondary reactions at high temperatures become the main factor affecting the distribution of pyrolysis products, prompting the decomposition of long chains into short-chain hydrocarbons as the temperature increases.

It can be seen from the variation of the reaction equilibrium constant with the pressure that the increase in pressure is not favorable for the reaction to proceed. Compared with atmospheric pressure, the temperatures at which the Gibbs free energies of reactions R4 and R5 are less than 0 are increased by 27 and 24 °C, respectively, at a pressure of 10 MPa, again moving to a higher-temperature gradient to some extent. Previous research reported that the mass fraction of aliphatic hydrocarbon compounds in tar decreased from 29.93 to 27.80% as the pyrolysis pressure increased from 1 MPa to 4 MPa at a pyrolysis temperature of 600 °C.[60] The reason may be that the increase in pressure leads to the cleavage of aliphatic hydrocarbon compounds into short-chain compounds and small molecules of alkane gas. Therefore, the pressure on the aliphatic hydrocarbon fraction during pyrolysis may affect the production and release of products by breaking fatty side chains in coal and cleaving aliphatic compounds.

3.3. Thermodynamic Analysis of Typical Components of Phenolic Oils. From the change of Gibbs free energy with temperature for the *in situ* underground pyrolysis of tar-rich coal to generate phenolic fractions in one reaction in Figure 7, it can be seen that reactions R6, R7, and R8 can proceed spontaneously at atmospheric pressure in the temperature intervals of 284, 311, and above 416 °C, respectively. From the change of the equilibrium constant of the reaction with temperature, it can be seen that the equilibrium constant increases with an increase of temperature, so the reactions are all heat-absorbing reactions, and the increase in temperature is

https://doi.org/10.1021/acsomega.3c01321
ACS Omega 2023, 8, 18915−18929

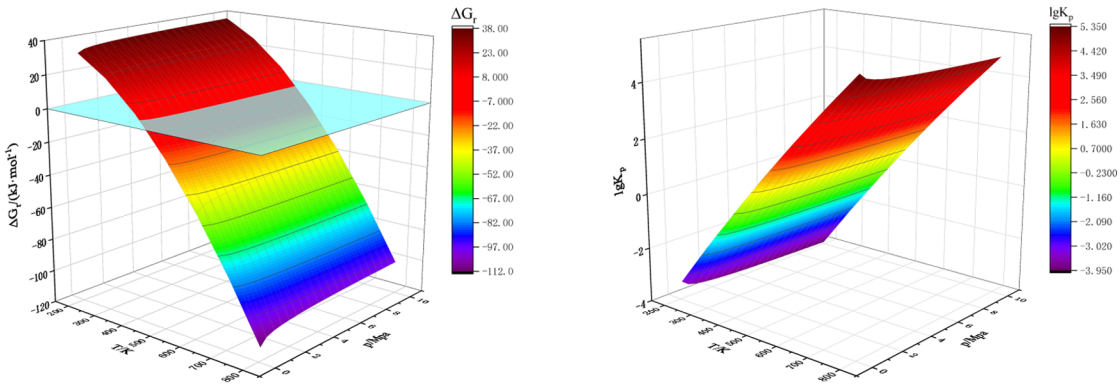

$$CH_{0.761}O_{0.273}N_{0.01}S_{0.005} \rightarrow 0.1252C_6H_5OH+0.005N_2+0.005H_2S+0.101C+0.1478CO$$

(a) R6- The change of Gibbs free energy (b) R6- Equilibrium constant

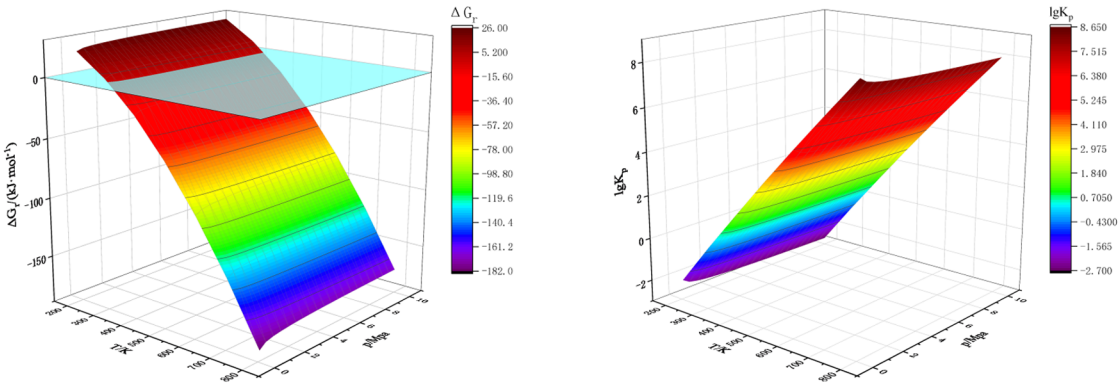

$$CH_{0.761}O_{0.273}N_{0.01}S_{0.005} \rightarrow 0.0939C_6H_4CH_3OH+0.005N_2+0.005H_2S+0.1636C+0.1791CO$$

(c) R7- The change of Gibbs free energy (d) R7- Equilibrium constant

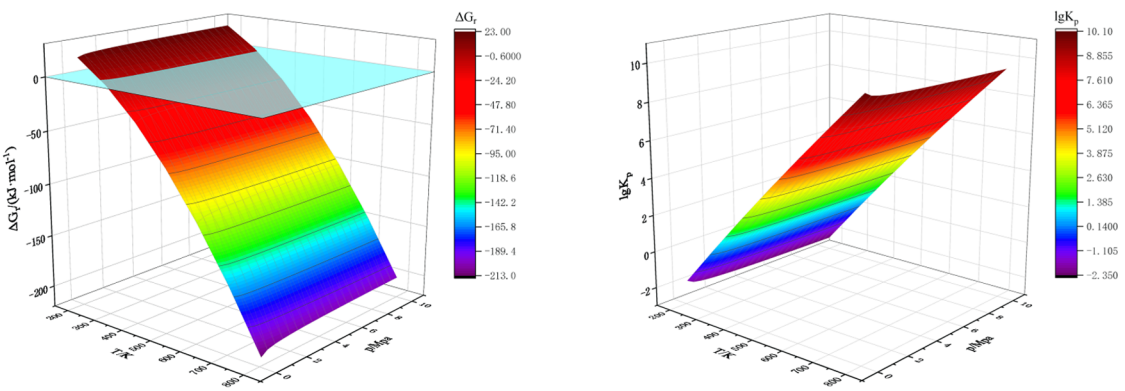

$$CH_{0.761}O_{0.273}N_{0.01}S_{0.005} \rightarrow 0.0751C_6H_3(CH_3)_2OH+0.005N_2+0.005H_2S+0.2013C+0.1979CO$$

(e) R8- The change of Gibbs free energy (f) R8- Equilibrium constant

Figure 7. Effects of temperature and pressure on the change of the Gibbs free energy and equilibrium constant of phenol oil components.

favorable for the positive proceeding of the reaction. Phenolic compounds mainly come from the thermal decomposition of oxygenated compounds during coal pyrolysis, and the breakage of −OH, −C═O, and aryl ether bonds is the main source of phenolic compounds.[61] The production of phenolic compounds tends to increase and then decrease as the pyrolysis temperature increases.[62,63] It was reported that when the pyrolysis temperature was increased from 700 to 900 °C, the content of phenol in tar decreased from 12.8 to 0.9%.[64] In a previous study, related scholars found that the production of phenol in tar reached a maximum at 700 °C, after which the breakage of $-CH_3$ and phenol−OH mainly occurred, resulting in a decrease in the production of phenolic compounds.[65] Therefore, at low temperatures, the increase in temperature led to a large number of $-CH_3$ and aromatic ether bond breaks, increasing the phenolic compound content, which is consistent with literature reports; in contrast, the deviation at high temperatures was mainly because above 700 °C; the coal

https://doi.org/10.1021/acsomega.3c01321
ACS Omega 2023, 8, 18915−18929

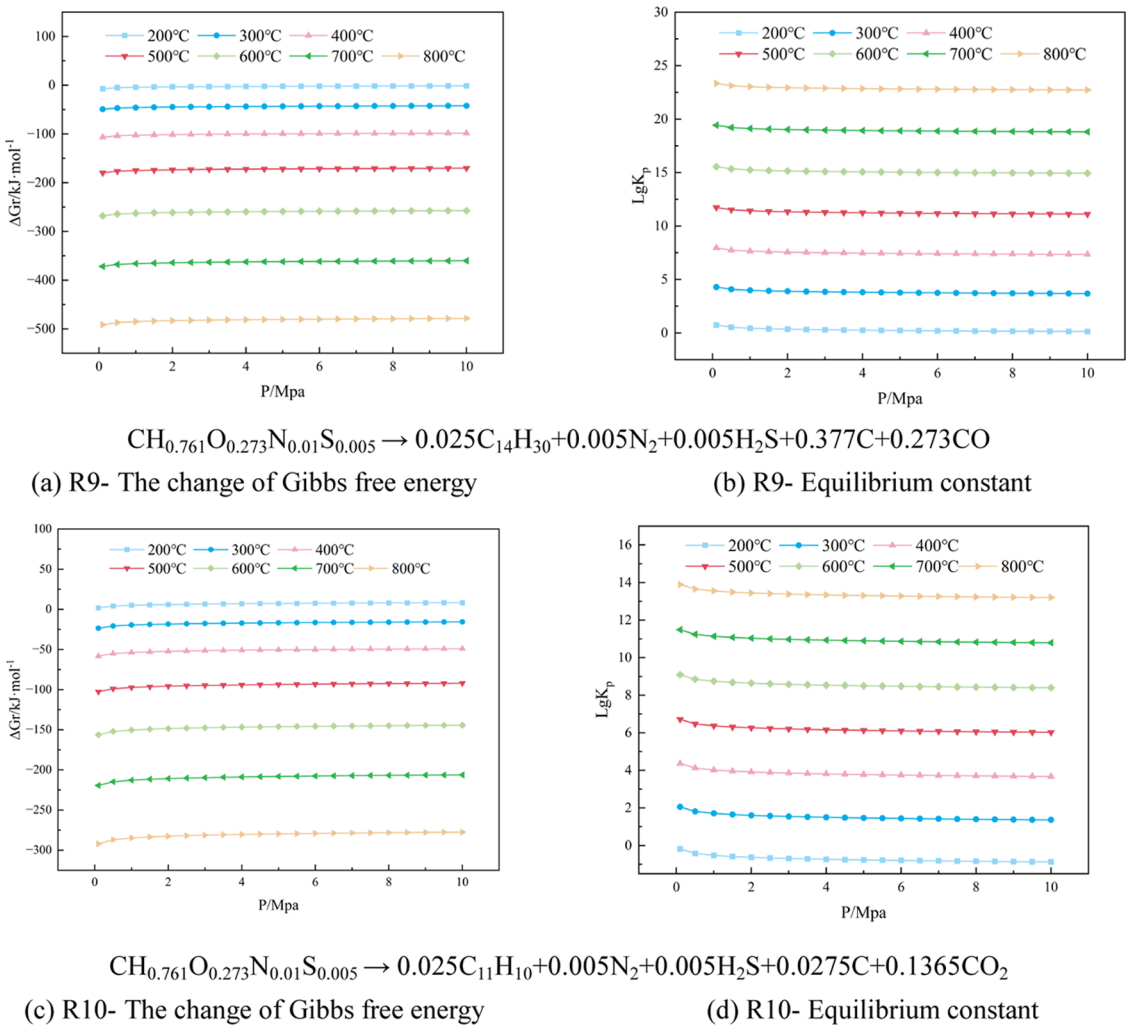

Figure 8. Effects of temperature and pressure on the change of the Gibbs free energy and equilibrium constant of oil washing components.

pyrolysis reaction was dominated by condensation reactions; and the phenolic compounds underwent cleavage, dehydroxylation reactions, and other reactions, leading to a decrease in content.

The variation of the reaction equilibrium constant with pressure shows that the increase of pressure is not favorable for the reaction. At a pressure of 10 MPa, the reaction free energies of reactions R6, R7, and R8 are less than 0 at 311, 342, and 454 °C, respectively, which are increased by 58 °C, 31 °C, and 38 °C, respectively, compared with atmospheric pressure; thus, the temperature at which the reaction starts is similarly shifted to higher temperatures under subsurface stress. It has been shown that under 700 °C, the production of phenolic compounds tended to increase with increasing pyrolysis pressure.[66] Similar results were found by related authors who studied the effect of pressure on the pyrolysis of palm shells, where the phenolic content increased with increasing pressure at lower temperatures, while above 800 °C, the phenolic content decreased rapidly with increasing pressure, probably due to the conversion of phenol to benzene or benzene radicals.[67] The main reason for the deviation may be that the increase in pressure is not conducive to the primary reaction, and the actual analysis should be combined with the cracking of phenolic compounds to analyze the generation and release of phenolic oil components.

3.4. Thermodynamic Analysis of Typical Components of the Washed Oil Fraction. From the change of the Gibbs free energy of primary reactions with temperature in Figure 8, it can be seen that the free energies of reactions R9 and R10 were generated at atmospheric pressure with free energy less than 0 above 204 and 234 °C, respectively. These reactions can proceed spontaneously in this temperature range. The variation of the equilibrium constant of the reaction with temperature shows that the equilibrium constant increases with increasing temperature, so the reactions are all heat-absorbing reactions, and the positive proceeding of the reaction is favored with increasing temperature. The generative mechanism of tetradecane is similar to that of previous alkanes. Sun et al.[68] found that alkanes and olefins with fewer than 28 carbon atoms in the main chain may be produced by cracking large n-alkanes in coal. Liu et al.[51] found that the relative concentration of n-tetradecane decreased with an increase in temperature, while the relative concentrations of C_5H_{10}, C_6H_{12}, and C_1-C_3 alkyl radicals increased monotonically. Therefore, the increase in temperature leads to the decomposition of tetradecane into some small-molecular alkyl/alkenyl radicals and alkenes. The PAHs generated during coal pyrolysis are mainly from the cleavage reaction of large molecules and the condensation reaction of small molecules in raw coal.[69,70] The highest production of two-ring aromatic hydrocarbons was found at a

https://doi.org/10.1021/acsomega.3c01321
ACS Omega 2023, 8, 18915−18929

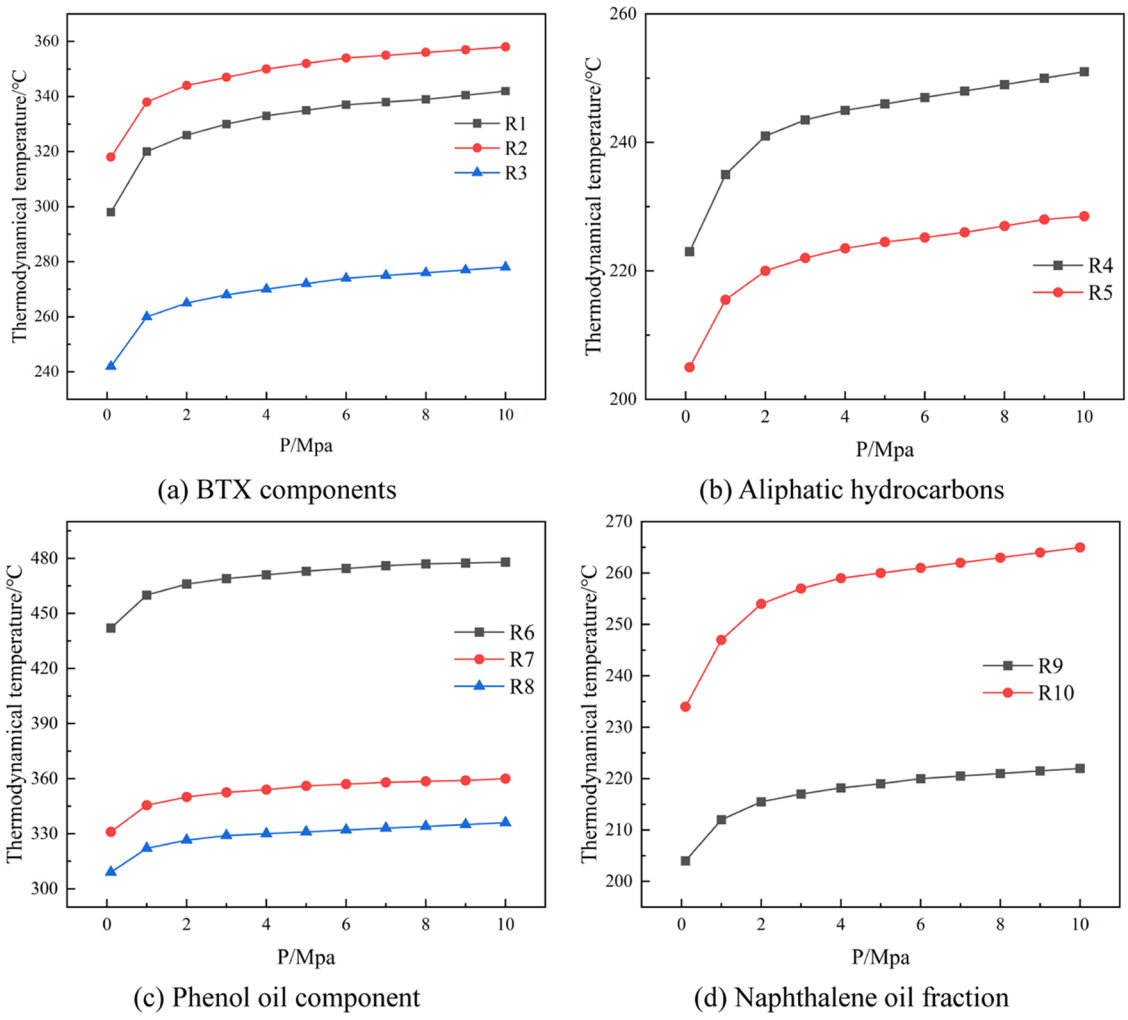

Figure 9. Thermodynamically feasible temperature of the reaction.

pyrolysis temperature of 400 °C, which then decreased with increasing temperature.[71] Kong et al.[72] studied the release pattern of PAHs from Pingshuo coal at different pyrolysis temperatures, and they found that the generation of two- to three-ring PAHs with small molecular weights was mainly concentrated at 600−800 °C because condensation reactions mainly dominated the later stages of pyrolysis. The small-ring PAHs underwent condensation reactions to generate large-molecular-weight PAHs at high temperatures. Consistent with the results of thermodynamic analysis, with the increase of pyrolysis temperature, the bridge bonds, aliphatic side chains on the aromatic ring, and methyl and phenolic hydroxyl groups in the coal structure were broken sequentially, which contributed to the increasing amount of PAH production.

From the variation of the reaction equilibrium constant with pressure, it can be seen that the reaction equilibrium constant decreases with an increase of pressure and is therefore not favorable for the reaction. Compared with atmospheric pressure, the thermodynamically feasible temperatures of reactions R9 and R10 increase by 19 and 31 °C, respectively, at a pressure of 10 MPa. The effect of subsurface stress drives the temperature at the beginning of the primary pyrolysis reaction to a higher-temperature gradient. The effect of pressure on tetradecane is the same as that in Section 3.2.2. This section mainly discusses the effect of pressure on methylnaphthalene. It has been reported that the concentration of naphthalene and its derivatives in tar increases with increasing pressure at 600 °C,[58] which is different from the results of thermodynamic analysis, mainly because the volatile fraction is retained longer in the semicoke at high pressure and the thermal cleavage of the monocyclic units in the macromolecular structure of lignite leads to the formation of phenyl and naphthalene radicals, which can be further grown by the HACA mechanism to form radicals with 2−5 rings of polycyclic aromatic hydrocarbons these intermediate radicals produce polycyclic aromatic hydrocarbons by addition reaction with acetylene.[73,74] Therefore, the effect of pressure on polycyclic aromatic hydrocarbons such as dimethyl naphthalene should be analyzed comprehensively.

As shown in Figure 9, the thermodynamically feasible initial temperature of the primary reaction of each component at a reaction pressure of 10 MPa shows different degrees of increase. For light oil components, the content of alkanes in light oil accounts for about 10%, the content of aromatic hydrocarbons accounts for 30−40%,[68] and the relative content of xylene is greater than that of toluene and benzene, with an increase of reaction pressure.[45] On the other hand, the thermodynamically feasible temperature change of reaction R3 has less influence than that of reactions R1 and R2. Therefore, among the five reactions that generate light oil, reaction R3 plays a leading role in the *in situ* conditions. In phenolic oil, the content of phenol is 5−10%, the content of cresol is 30%, and

https://doi.org/10.1021/acsomega.3c01321
ACS Omega 2023, 8, 18915−18929

the content of xylenol is 25%.[75] The initial temperature of reactions R7 and R8 is lower than that of reaction 6, and the change with the increase of pressure is small. Therefore, reactions R6 and R7 play a more important role in phenolic oil. The mass fraction of methylnaphthalene in wash oil is 20−25%,[76] and the thermodynamically feasible temperature of reactions R9 and R10 changes little with pressure, so reaction R10 has a greater influence on wash oil components. For the optimal temperature−pressure interval of product generation, it is also necessary to discriminate the influence of thermodynamic calculations of the secondary reactions of coal pyrolysis on the components.

4. CONCLUSIONS

A thermodynamic study of *in situ* underground pyrolysis of tar-rich coal was carried out for the reaction characteristics and pyrolysis behavior under a typical tar-rich coal *in situ* environment. Thermodynamic functions, including the standard enthalpy of formation $\Delta H_f^{\ominus}$, standard formation Gibbs free energy $\Delta G_f^{\ominus}$, and standard entropy $\Delta S_m^{\ominus}$, were determined to analyze the components of washed oil, phenol oil, and light oil produced by the primary reaction of tar-rich coal pyrolysis and the variation of the free energy of the primary reaction of pyrolysis under the temperature from 200 to 800 °C and pressure from atmospheric pressure to 10 MPa. The thermodynamic functions of typical tar-rich coals were determined under standard conditions: the standard enthalpy of formation of tar-rich coals was −72.27 kJ·mol^{-1}, and the standard entropy was −37.79 J·mol^{-1}·K^{-1}, and the standard formation Gibbs free energy was −60.01 kJ·mol^{-1}. From the product tar fraction, different pyrolysis primary reactions of tar-rich coals were constructed and studied at 200−800 °C and atmospheric pressure−10 MPa, the variation of reaction thermodynamic parameters with temperature and pressure was investigated, and the results showed that the increase of temperature was favorable for the primary pyrolysis reaction. In contrast, the increase in pressure was unfavorable for the primary reaction. In the 500 m subsurface *in situ* underground pyrolysis, the thermodynamically feasible initial temperatures of the primary reaction increased by 45, 38, 36, 27 °C, and 24 °C for the light oil fraction; 58, 31, and 38 °C for the phenol oil fraction; and 19 and 31 °C for the washed oil fraction. In the 500 m subsurface environment, the temperature at which the primary reaction of *in situ* pyrolysis began moved to a higher-temperature gradient.

AUTHOR INFORMATION

Corresponding Author

Zhiqiang Wu − *Shaanxi Provincial Coal Geology Group Co. Ltd., Xi'an, Shaanxi 710054, P. R. China; Key Laboratory of Coal Resources Exploration and Comprehensive Utilization, Ministry of Natural Resources, Xi'an, Shaanxi 710026, P. R. China; Shaanxi Key Laboratory of Energy Chemical Process Intensification, School of Chemical Engineering and Technology, Xi'an Jiaotong University, Xi'an, Shaanxi 710049, P. R. China;* orcid.org/0000-0002-3067-014X; Phone: +86-29-82665836; Email: zhiqiang-wu@mail.xjtu.edu.cn

Authors

Fu Yang − *Shaanxi Provincial Coal Geology Group Co. Ltd., Xi'an, Shaanxi 710054, P. R. China; Key Laboratory of Coal Resources Exploration and Comprehensive Utilization, Ministry of Natural Resources, Xi'an, Shaanxi 710026, P. R. China*

Kun Gao − *Shaanxi Key Laboratory of Energy Chemical Process Intensification, School of Chemical Engineering and Technology, Xi'an Jiaotong University, Xi'an, Shaanxi 710049, P. R. China*

Zunyi Yu − *Shaanxi Key Laboratory of Energy Chemical Process Intensification, School of Chemical Engineering and Technology, Xi'an Jiaotong University, Xi'an, Shaanxi 710049, P. R. China*

Li Ma − *Shaanxi Provincial Coal Geology Group Co. Ltd., Xi'an, Shaanxi 710054, P. R. China; Key Laboratory of Coal Resources Exploration and Comprehensive Utilization, Ministry of Natural Resources, Xi'an, Shaanxi 710026, P. R. China*

Husheng Cao − *Shaanxi Provincial Coal Geology Group Co. Ltd., Xi'an, Shaanxi 710054, P. R. China; Key Laboratory of Coal Resources Exploration and Comprehensive Utilization, Ministry of Natural Resources, Xi'an, Shaanxi 710026, P. R. China*

Panxi Yang − *Shaanxi Key Laboratory of Energy Chemical Process Intensification, School of Chemical Engineering and Technology, Xi'an Jiaotong University, Xi'an, Shaanxi 710049, P. R. China*

Wei Guo − *Shaanxi Key Laboratory of Energy Chemical Process Intensification, School of Chemical Engineering and Technology, Xi'an Jiaotong University, Xi'an, Shaanxi 710049, P. R. China*

Jie Zhang − *Shaanxi Key Laboratory of Energy Chemical Process Intensification, School of Chemical Engineering and Technology, Xi'an Jiaotong University, Xi'an, Shaanxi 710049, P. R. China*

Bolun Yang − *Shaanxi Key Laboratory of Energy Chemical Process Intensification, School of Chemical Engineering and Technology, Xi'an Jiaotong University, Xi'an, Shaanxi 710049, P. R. China*

Complete contact information is available at: https://pubs.acs.org/10.1021/acsomega.3c01321

Author Contributions

‖F.Y. and K.G. contribute equally to this paper.

Notes

The authors declare no competing financial interest.

ACKNOWLEDGMENTS

The financial support from the Research Project of Shaanxi Provincial Coal Geology Group Co. Ltd. (Nos. SMDZ-2020ZD-1-02,SMDZ-2020ZD-1-06), the K.C. Wong Education Foundation, Shaanxi Province Qin Chuangyuan "Scientist + Engineer" team development project (No. 2022KXJ-126), and the Innovation Capability Support Program of Shaanxi (Program Nos. 2022KJXX-24,2023KJXX-004,2023-CX-TD-26) is acknowledged.

SYMBOL DESCRIPTION TABLE

C_p	heat capacity at constant pressure, J·kg^{-1}·K^{-1}
G	Gibbs free energy, kJ·mol^{-1} G_0 initial Gibbs free energy of tar-rich coal T0 the ambient temperature /298.15K
H	enthalpy, kJ·mol^{-1}
$\Delta_D H$	bond energy, kJ·mol^{-1}
M_a	average molecular weight
Q	combustion heat, MJ·kg^{-1}

https://doi.org/10.1021/acsomega.3c01321
ACS Omega 2023, 8, 18915−18929

S entropy, $J \cdot mol^{-1} \cdot K^{-1}$
T_i dissociation temperature, K
$T_D K$ maximum dissociation temperature, K
v_i number of chemical measures
X_i chemical bonding ratio
x_i mass fraction of components, %
δ_v vertical stress, MPa
$\ominus$ standard state
a average
α molar ratio
f generate state
i component
r reactive state
v vertical direction G_0 the initial Gibbs free energy of tar-rich coal,Gibbs free energy, $kJ \cdot mol^{-1}$; T_0 the ambient temperature, K

REFERENCES

(1) BP. *Statistical Review of World Energy 2021*; British Petroleum (BP): London, 2021.
(2) Yearbook, E. C. o. C. E. *China Energy Yearbook 2021*; Science Press: Beijing, 2022.
(3) Wang, S.-M. Thoughts about the main energy status of coal and green mining in China. *China Coal* **2020**, *46*, 11−16.
(4) CNPC. *Domestic and International Oil and Gas Industry Development Report in 2021*; Petroleum Industry Press: Beijing, 2022.
(5) Committee, M. R. I. R. M. E. *Mineral Resources Industry Requirements Manual*; Geology Press: Beijing, 2014.
(6) Wang, S.-M.; Shi, Q.-M.; Wang, S.-Q. Resource property and exploitation concepts with green and low-carbon of tar-rich coal as coal-based oil and gas. *J. China Coal Soc.* **2021**, *46*, 1365−1377.
(7) Zhang, N.; Xu, Y.; Qiao, J.; Ning, S. Organic geochemistry of the Jurassic tar-rich coal in Northern Shaanxi Province. *Coal Geol. Explor.* **2021**, *49*, 42−49.
(8) Zhao, H.; Li, Y.; Song, Q.; Liu, S.; Yan, J.; Ma, Q.; Ma, L.; Shu, X. Investigation on the thermal behavior characteristics and products composition of four pulverized coals: Its potential applications in coal cleaning. *Int. J. Hydrogen Energy* **2019**, *44*, 23620−23638.
(9) Xie, K.-C.; He, W. *Introduction to Coal Chemical Industry*; Chemical Industry Press: Beijing, 2012.
(10) Sathe, C.; Hayashi, J.-I.; Li, C.-Z. Release of volatiles from the pyrolysis of a Victorian lignite at elevated pressures. *Fuel* **2002**, *81*, 1171−1178.
(11) Matsuoka, K.; Ma, Z.-x.; Akiho, H.; Zhang, Z.-g.; Tomita, A.; Fletcher, T. H.; Wójtowicz, M. A.; Niksa, S. High-Pressure Coal Pyrolysis in a Drop Tube Furnace. *Energy Fuels* **2003**, *17*, 984−990.
(12) Cai, H. Y.; Guell, A. J.; Dugwell, D. R.; Kandiyoti, R. Heteroatom distribution in pyrolysis products as a function of heating rate and pressure. *Fuel* **1993**, *72*, 321−327.
(13) Cai, H. Y.; Güell, A. J.; Chatzakis, I. N.; Lim, J. Y.; Dugwell, D. R.; Kandiyoti, R. Combustion reactivity and morphological change in coal chars: Effect of pyrolysis temperature, heating rate and pressure. *Fuel* **1996**, *75*, 15−24.
(14) Niksa, S.; Liu, G. S.; Hurt, R. H. Coal conversion submodels for design applications at elevated pressures. Part I. Devolatilization and char oxidation. *Prog. Energy Combust. Sci.* **2003**, *29*, 425−477.
(15) Arendt, P.; van Heek, K. H. Comparative investigations of coal pyrolysis under inert gas and H2 at low and high heating rates and pressures up to 10 MPa. *Fuel* **1981**, *60*, 779−787.
(16) Gibbins, J. R.; Gonenc, Z. S.; Kandiyoti, R. Pyrolysis and hydropyrolysis of coal: comparison of product distributions from a wire-mesh and a hot-rod reactor. *Fuel* **1991**, *70*, 621−626.
(17) Guell, A. J.; Kandiyoti, R. Development of a gas-sweep facility for the direct capture of pyrolysis tars in a variable heating rate high-pressure wire-mesh reactor. *Energy Fuels* **1993**, *7*, 943−952.
(18) Liu, X.; Peng, J. Study on the tar structure and nature of pressurized pyrolysis for Tianzhu coal in Gansu. *Coal Conversion* **1994**, *17*, 82−88.
(19) Messenböck, R.; Dugwell, D. R.; Kandiyoti, R. CO_2 and steam-gasification in a high-pressure wire-mesh reactor: the reactivity of Daw Mill coal and combustion reactivity of its chars. *Fuel* **1999**, *78*, 781−793.
(20) Messenböck, R. C.; Dugwell, D. R.; Kandiyoti, R. Coal Gasification in CO2 and Steam: Development of a Steam Injection Facility for High-Pressure Wire-Mesh Reactors. *Energy Fuels* **1999**, *13*, 122−129.
(21) Seebauer, V.; Petek, J.; Staudinger, G. Effects of particle size, heating rate and pressure on measurement of pyrolysis kinetics by thermogravimetric analysis. *Fuel* **1997**, *76*, 1277−1282.
(22) Sharma, D. K.; Sulimma, A.; van Heek, K. H. Hydropyrolysis of coal in the presence of steam. *Fuel* **1986**, *65*, 1571−1574.
(23) Van Heek, K. H.; Hodek, W. Structure and pyrolysis behaviour of different coals and relevant model substances. *Fuel* **1994**, *73*, 886−896.
(24) Xie, X.; Liu, L.; Lin, D.; Zhao, Y.; Qiu, P. Influence of different state alkali and alkaline earth metal on chemical structure of Zhundong coal char pyrolyzed at elevated pressures. *Fuel* **2019**, *254*, No. 115691.
(25) Xu, W.-C.; Matsuoka, K.; Akiho, H.; Kumagai, M.; Tomita, A. High pressure hydropyrolysis of coals by using a continuous free-fall reactor. *Fuel* **2003**, *82*, 677−685.
(26) Zhao, L. *Study on Characteristics of Coal Pyrolysis under Different Conditions and Mechanism of Catalyst Used in Pyrolysis*; Zhejiang University, 2017.
(27) Gibbins, J. R.; Kandiyoti, R. The effect of variations in time-temperature history on product distribution from coal pyrolysis. *Fuel* **1989**, *68*, 895−903.
(28) Zhang, S.; He, R. Secondary reactions and diffusion of tar during single coal particle pyrolysis. *Qinghua Daxue Xuebao* **2016**, *56*, 605−610.
(29) Chen, J. C.-Y. Effects of Secondary Reactions on Product Distribution and Nitrogen Evolution from Rapid Coal Pyrolysis, Ph.D., Stanford University: Ann Arbor, 1991.
(30) Smith, P. J.; Deo, M.; Edding, E. G.; Hradisky, M.; Kelly, K. E.; Krumm, R.; Sarofim, A.; Wang, D. *Underground Coal Thermal Treatment: Task 6 Topical Report, Utah Clean Coal Program*; University of Utah: Salt Lake City, UT (United States), 2014.
(31) Wang, D.; Fletcher, T. H.; Mohanty, S.; Hu, H.; Eddings, E. G. Modified CPD Model for Coal Devolatilization at Underground Coal Thermal Treatment Conditions. *Energy Fuels* **2019**, *33*, 2981−2993.
(32) Kelly, K. E.; Wang, D.; Hradisky, M.; Silcox, G. D.; Smith, P. J.; Eddings, E. G.; Pershing, D. W. Underground coal thermal treatment as a potential low-carbon energy source. *Fuel Process Technol.* **2016**, *144*, 8−19.
(33) Zhang, H. R.; Li, S.; Kelly, K. E.; Eddings, E. G. Underground in situ coal thermal treatment for synthetic fuels production. *Prog. Energy Combust. Sci.* **2017**, *62*, 1−32.
(34) Feng, Z.; Wan, Z.; Zhao, Y.; Li, G.; Zhang, Y.; Wang, C.; Zhu, N. Experimental study of the permeability of anthracite and gas coal masses under high temperature and triaxial stress. *Chin. J. Rock Mech. Eng.* **2010**, *29*, 686−696.
(35) Shao, J.; Hu, Y.; Meng, T.; Song, S.; Jin, P.; Feng, G. Effect of Temperature on Permeability and Mechanical Characteristics of Lignite. *Adv. Mater. Sci. Eng.* **2016**, *2016*, 1−12.
(36) Niu, S.; Zhao, Y.; Hu, Y. Experimental Ivestigation of the Temperature and Pore Pressure Effect on Permeability of Lignite Under the In Situ Condition. *Transp. Porous Media* **2014**, *101*, 137−148.
(37) Duan, T.-H.; Wang, Z.-T.; Liu, Z.-J.; Chen, Y.-Z.; Fu, Z.-B. Experimental Study of Coal Pyrolysis under the Simulated High Temperature and High-Stress Conditions of Underground Coal Gasification. *Energy Fuels* **2017**, *31*, 1147−1158.

https://doi.org/10.1021/acsomega.3c01321
ACS Omega 2023, 8, 18915−18929

(38) Cheng, X.-L.; Fan, T.-F.; Du, P.-F.; Tian, W.-D.; Xiao, Y.-H. Thermodynamic Analysis of Direct Methane Production From Coal. *J. Eng. Thermophys.* **2012**, *33*, 1647−1650.
(39) Lv, Y.-K.; Pang, X. Y.; Bao, W.-R.; Xie, K.-C. Coal pyrolysis in plasma and thermodynamic analysis for model compound. *J. Fuel Chem. Technol.* **2001**, *29*, 65−69.
(40) Atkins, P.; Atkins, P. W.; de Paula, J. *Atkins' Physical Chemistry*; Oxford University Press, 2014.
(41) Chen, W.-M. *Calorific Value of Coal and Calculation Formula*; China Coal Industry Publishing House: Beijing, 1997.
(42) Shinn, J. H. From coal to single-stage and two-stage products: A reactive model of coal structure. *Fuel* **1984**, *63*, 1187−1196.
(43) Xie, Kc. *Structure and Reactivity Of Coal*; Science Press: Beijing, 2002.
(44) GAO, C.; MA, F.-y.; MA, K.-j.; HUANG, L.-m.; ZHONG, M. Effect of pyrolysis gas on the tar quality from coal catalytic pyrolysis. *J. China Coal Soc.* **2015**, *15*, 1956−1962.
(45) Zhou, Y.; Li, L.; Jin, L.; Zhu, J.; Li, J.; Li, Y.; Fan, H.; Hu, H. Effect of functional groups on volatile evolution in coal pyrolysis process with in-situ pyrolysis photoionization time-of-flight mass spectrometry. *Fuel* **2020**, *260*, No. 116322.
(46) He, Q.; Wan, K.; Hoadley, A.; Yeasmin, H.; Miao, Z. TG−GC−MS study of volatile products from Shengli lignite pyrolysis. *Fuel* **2015**, *156*, 121−128.
(47) Xiong, Y.; Jin, L.; Li, Y.; Zhou, Y.; Hu, H. Structural Features and Pyrolysis Behaviors of Extracts from Microwave-Assisted Extraction of a Low-Rank Coal with Different Solvents. *Energy Fuels* **2019**, *33*, 106−114.
(48) Zhan, J.-H.; Wu, R.; Liu, X.; Gao, S.; Xu, G. Preliminary understanding of initial reaction process for subbituminous coal pyrolysis with molecular dynamics simulation. *Fuel* **2014**, *134*, 283−292.
(49) Zheng, M.; Li, X.; Wang, M.; Guo, L. Dynamic profiles of tar products during Naomaohu coal pyrolysis revealed by large-scale reactive molecular dynamic simulation. *Fuel* **2019**, *253*, 910−920.
(50) Qian, Y.; Zhan, J.-H.; Xu, W.; Han, Z.; Liu, X.; Xu, G. ReaxFF molecular dynamic simulation of primary and secondary reactions involving in sub-bituminous coal pyrolysis for tar production. *Carbon Resources Conversion* **2021**, *4*, 230−238.
(51) Liu, F.; Jin, L.; Ban, Y.; Hu, H. Study on pyrolysis behavior of long-chain n-alkanes with photoionization molecular-beam mass spectrometer. *J. Anal. Appl. Pyrolysis* **2021**, *159*, No. 105324.
(52) SHI, Q.; WANG, S.; WANG, S.; Guo, C.; CAI, Y.; DU, F.-p.; QIAO, J.; CHANG, B.; ZHANG, H.; MIAO, Y. Multi-source identification and internal relationship of tar-rich coal of the Yan'an Formation in the south of Shenfu. *J. China Coal Soc.* **2021**, *47*, 10.
(53) Kang, H.-P.; YI, B.-D.; Gao, F.-Q.; Lv, H.-W. Database and characteristics of underground in-situ stress distribution in Chinese coal mines. *J. China Coal Soc.* **2019**, *44*, 23−33.
(54) Burnham, A. K.; Oh, M. S.; Crawford, R. W.; Samoun, A. M. Pyrolysis of Argonne premium coals: activation energy distributions and related chemistry. *Energy Fuels* **1989**, *3*, 42−55.
(55) Nyakuma, B. B.; Jauro, A.; Akinyemi, S. A.; Faizal, H. M.; Nasirudeen, M. B.; Fuad, M.; Oladokun, O. Physicochemical, mineralogy, and thermo-kinetic characterisation of newly discovered Nigerian coals under pyrolysis and combustion conditions. *Int. J. Coal Sci. Technol.* **2021**, *8*, 697−716.
(56) Chen, X.-Y.; Wang, Q.-H.; Cen, J.-M.; Guo, Z.-H.; Fang, M.-X.; Luo, Z.-Y. Efect of Temperature on Pyrolysis Products of Xiaolongtan Lignite in a Fluidized-bed Reactor. *J. Chin. Soc. Power Eng.* **2011**, *31*, 316−320.
(57) Cor, J.; Manton, N.; Mul, G.; Eckstrom, D.; Olson, W.; Malhotra, R.; Niksa, S. An Experimental Facility for the Study of Coal Pyrolysis at 10 Atmospheres. *Energy Fuels* **2000**, *14*, 692−700.
(58) Tahmasebi, A.; Maliutina, K.; Matamba, T.; Kim, J.-H.; Jeon, C.-H.; Yu, J. Pressurized entrained-flow pyrolysis of lignite for enhanced production of hydrogen-rich gas and chemical raw materials. *J. Anal. Appl. Pyrolysis* **2020**, *145*, No. 104741.
(59) Lievens, C.; Ci, D.; Bai, Y.; Ma, L.; Zhang, R.; Chen, J. Y.; Gai, Q.; Long, Y.; Guo, X. A study of slow pyrolysis of one low rank coal via pyrolysis−GC/MS. *Fuel Process Technol* **2013**, *116*, 85−93.
(60) Wang, N.; Huang, Y.; Liu, Q.; Zhang, Y.; Yang, H. Effects of Pyrolysis Conditions on Pressurized Pyrolysis of Xiwan Coal in Fluidized Bed. *Coal Conversion* **2021**, *44*, 34−43.
(61) Siskin, M.; Aczel, T. Pyrolysis studies on the structure of ethers and phenols in coal. *Fuel* **1983**, *62*, 1321−1326.
(62) Li, G.; Li, L.; Shi, L.; Jin, L.; Tang, Z.; Fan, H.; Hu, H. Experimental and Theoretical Study on the Pyrolysis Mechanism of Three Coal-Based Model Compounds. *Energy Fuels* **2014**, *28*, 980−986.
(63) Ge, Y. Phenolic compounds in the liquid products produce during coal pyrolysis at low-temperature part (I) producing mechanism. *Coal Conversion* **1997**, *20*, 14−19.
(64) Dong, L.; Han, S.; Yu, W.; Lei, Z.; Kang, S.; Zhang, K.; Yan, J.; Li, Z.; Shui, H.; Wang, Z.; Ren, S.; Pan, C. Effect of volatile reactions on the yield and quality of tar from pyrolysis of Shenhua bituminous coal. *J. Anal. Appl. Pyrolysis* **2019**, *140*, 321−330.
(65) Kong, J.; Zhao, R.; Bai, Y.; Li, G.; Zhang, C.; Li, F. Study on the formation of phenols during coal flash pyrolysis using pyrolysis-GC/MS. *Fuel Process Technol.* **2014**, *127*, 41−46.
(66) Zhang, C.; Zhu, S.; Bai, Y.; Liu, C. Effect of CO_2 on phenolic compounds distribution during Yining coal pyrolysis. *Coal Conversion* **2015**, *38*, 17−22.
(67) Matamba, T.; Tahmasebi, A.; Khoshk Rish, S.; Yu, J. Promotion Effects of Pressure on Polycyclic Aromatic Hydrocarbons and H2 Formation during Flash Pyrolysis of Palm Kernel Shell. *Energy Fuels* **2020**, *34*, 3346−3356.
(68) Sun, M.; Zhang, D.; Yao, Q.; Liu, Y.; Su, X.; Jia, C. Q.; Hao, Q.; Ma, X. Separation and Composition Analysis of GC/MS Analyzable and Unanalyzable Parts from Coal Tar. *Energy Fuels* **2018**, *32*, 7404−7411.
(69) Dong, J.; Li, F.; Xie, K. Study on the source of polycyclic aromatic hydrocarbons (PAHs) during coal pyrolysis by PY−GC−MS. *J. Hazard. Mater.* **2012**, *243*, 80−85.
(70) Liu, J.; Zhao, W.; Fan, X. R.; Xu, M. X.; Zheng, S.; Lu, Q. Effect of alkali metal ions on the formation mechanism of HCN during pyridine pyrolysis. *Int. J. Coal Sci. Technol.* **2021**, *8*, 349−359.
(71) Liu, S.-Q.; Jin, Z.-W.; Zhang, S.-J.; Wang, Y.-Y.; LI, Y.-H.; Zeng, Y.-J.; Zhang, Y.; Yi, R.; Li, X.-X. Formation and distribution of polycyclic aromatic hydrocarbons during large size coal pyrolysis. *J. China Coal Soc.* **2012**, *37*, 1039−1045.
(72) Kong, J.; Cheng, Z.; Dong, J.; Jiao, H.-l.; Li, F. Release of PAHs during pyrolysis of Pingshuo coal. *J. Fuel Chem. Technol.* **2013**, *41*, 1281−1286.
(73) Shukla, B.; Koshi, M. A novel route for PAH growth in HACA based mechanisms. *Combust. Flame* **2012**, *159*, 3589−3596.
(74) Frenklach, M.; Wang, H. Detailed modeling of soot particle nucleation and growth. *Symp. Int. Combust.* **1991**, *23*, 1559−1566.
(75) Xu, C. Characteristics and processing utilization of coal tar. *Clean Coal Technology* **2013**, *19*, 5.
(76) Huang, Y.; Feng, J.; Liang, C.-H.; Huang, P.; Zhang, X.-W.; Xie, Q.; Li, W.-Y. Co-production of Naphthenic Oil and Phenolic Compounds from Medium- and Low-Temperature Coal Tar. *Ind. Eng. Chem. Res.* **2021**, *60*, 5890−5902.

https://doi.org/10.1021/acsomega.3c01321
ACS Omega 2023, 8, 18915−18929